Available online at www.sciencedirect.com
SCIENCE DIRECT
DNA Repair 4 (2005) 1314–1324
DNA REPAIR
www.elsevier.com/locate/dnarepair

Accelerated aging pathology in ad libitum fed Xpd^{TTD} mice is accompanied by features suggestive of caloric restriction

Susan W.P. Wijnhoven [a], Rudolf B. Beems [a], Marianne Roodbergen [a], Jolanda van den Berg [a], Paul H.M. Lohman [a], Karin Diderich [b], Gijsbertus T.J. van der Horst [b], Jan Vijg [c], Jan H.J. Hoeijmakers [b], Harry van Steeg [a,*]

[a] *National Institute of Public Health and the Environment, Laboratory of Toxicology, Pathology and Genetics, Bilthoven, The Netherlands*
[b] *MGC-Department of Cell Biology and Genetics, Center for Biomedical Genetics, Erasmus University Medical Center, Rotterdam, The Netherlands*
[c] *Department of Physiology and Barshop Center for Longevity and Aging Studies, University of Texas Health Science Center, San Antonio, TX, USA*

Received 19 April 2005; received in revised form 6 July 2005; accepted 6 July 2005
Available online 22 August 2005

Abstract

Trichothiodystrophy (TTD) patients with a mutation in the *XPD* gene of nucleotide excision repair (NER) have a short life span and show various features of premature aging, thereby linking DNA damage to the aging process. Xpd^{TTD} mutant mice share many features with TTD patients, including a shorter life span, accompanied by a segmental progeroid phenotype. Here we report new pathology features supportive to the premature aging phenotype of Xpd^{TTD} mice. Strikingly, accelerated aging pathology is accompanied by signs suggestive of caloric restriction (CR), a condition usually linked to retardation of age-related pathology and life extension. Accelerated aging symptoms in Xpd^{TTD} mice are most likely due to accumulation of endogenously generated DNA damage and compromised transcription leading to cell death, whereas CR symptoms may reflect the need of Xpd^{TTD} mice to reduce metabolism (ROS production) in an attempt to extend their life span. Our current findings in Xpd^{TTD} mice further strengthen the link between DNA damage, repair and aging.

Keywords: Accelerated aging; Caloric restriction; Longevity study; Pathology features; Xpd^{TTD} mice

1. Introduction

Aging is a progressive, time-dependent deterioration in the capacity of an organism to properly function and respond adaptively to environmental challenges resulting in an increased vulnerability to death [1]. Within this process, cellular macromolecules like DNA, lipids and proteins accumulate damage leading to the malfunctioning of cellular organelles (like mitochondria) and cellular processes. In addition, damaged macromolecules may cause necrosis and apoptosis of cells resulting in tissue and organismal dysfunction, and therefore cans be considered as the ultimate driver of aging (reviewed in [2]). Damage to the genome leads to essentially irreversible loss of genetic information, and therefore will be more deleterious than damage to RNA, proteins or lipids that can be replaced [3]. A main source of spontaneous somatic DNA damage likely involves reactive oxygen species (ROS), natural by-products of normal oxidative energy metabolism [4,5]. More than 100 different types of oxidative DNA lesions have been described, ranging from base modifications to single- and double-strand DNA breaks and interstrand cross-links, DNA-protein crosslinks as well as damage to the phosphate-sugar backbone [6,7]. Oxidative DNA lesions might disrupt vital processes like transcription and replication, resulting in cell death or (transient or permanent) growth arrest or may induce mutations or chromosome aberrations that lead to cancer.

* Corresponding author. Tel.: +31 30 2742102; fax: +31 30 2744446.
E-mail address: h.van.steeg@rivm.nl (H. van Steeg).

1568-7864/$ – see front matter © 2005 Elsevier B.V. All rights reserved.
doi:10.1016/j.dnarep.2005.07.002

To counteract the effects of (oxidative) DNA damage, an intricate network of DNA repair pathways has evolved, each focusing on a different class of lesions. One major DNA repair pathway is nucleotide excision repair (NER), which removes a broad range of bulky lesions including UV-induced damage, chemical adducts as well as some forms of oxidative damage [7,8]. NER entails a complex 'cut and patch'-type reaction involving over 30 proteins. Important core components are the XPB and XPD helicases, which are subunits of the TFIIH complex implicated as DNA helix opener in both NER and in basal transcription initiation [9,10]. The multi-functionality of the XPD (and XPB) protein is further illustrated by the complex genotype–phenotype relationship in human NER patients with a mutation in *XPD*. Site-specific *XPD* mutations can lead to a variety of syndromes; xeroderma pigmentosum (XP), XP combined with Cockayne syndrome (CS), or trichothiodystrophy (TTD). XP patients are highly predisposed to (skin) cancer, CS and TTD patients show various features of premature aging whereas XP–CS patients display both [11,12].

The connection between NER deficiency and aging can be extended to several other DNA damage repair and response systems. Human segmental progeroid syndromes are frequently caused by genetic alterations that partially or wholly inactivate proteins that sense or repair DNA damage, like in the case of ataxia telangiectasia (AT), Bloom syndrome (BS) and Werner syndrome (WS) [13]. Hence, accelerated aging symptoms in both humans and mice with genetic defects in genome maintenance, strongly suggest that a wide-spread, strong connection exists between genome care-taking and accelerated aging [14].

In order to further investigate the causes and mechanisms that underlie the aging process and the influence of genome instability on this process, we are currently performing complete lifespan studies of various NER-deficient mouse strains, all defective in one or both sub-pathways of the NER repair system (i.e. *Xpa*, *Csb*, *Xpc* and Xpd^{TTD} mice) (reviewed in [15]). For these studies, the mouse mutants were backcrossed over 10 generations into a homogeneous C57BL/6 background and their survival was compared to wild type C57BL/6 controls under strict specific pathogen-free (SPF) conditions.

In this report, we focus on the previously described Xpd^{TTD} mouse model and its segmental progeroid phenotype. The results obtained in the present study confirm and significantly extend the previous observations on this mouse model [16]. Here we report many new features not reported before in Xpd^{TTD} females. While most of the new features involve additional symptoms of premature aging, we also report phenotypes, consistent with what is normally observed in mice during dietary/caloric restriction, an intervention that significantly increases lifespan and retards aging-related pathology [17]. This observed dichotomy in pathology of aging Xpd^{TTD} female mice might be related to the complex roles of the *Xpd* gene in both DNA repair and transcription.

2. Materials and methods

2.1. Mice

To perform longevity studies with extensive cohorts of homozygous mutant Xpd^{TTD} mice and C57BL/6 controls (Harlan), mice were passed through different rounds of breeding. Xpd^{TTD} mice used in this study carry a R722W mutation at the mouse *Xpd* gene. Generation of Xpd^{TTD} mice by targeting of the Xpd^{R722W} allele has been described previously [18]. To get a genetically homogenous background, Xpd^{TTD} mice were back-crossed over 10 times into a C57BL/6 background. To offer the future possibility to monitor genomic instability, heterozygous *Xpd* mutant mice as well as C57BL/6 controls were crossed with pUR288-*lacZ* C57BL/6 transgenic mice line 30, homozygous for *lacZ* integration on chromosome 11 [19], carrying 21 ± 1 copies of the pUR288-*lacZ* plasmid per haploid genome. In the second round of breeding, double heterozygous mice were intercrossed to obtain Xpd^{TTD} homozygous mice carrying one locus of the integrated copies of the *lacZ* marker, used in the third breeding round to generate the experimental animals for the aging (and interim) cohorts as described below. Mice were genotyped by a standard PCR reaction using DNA isolated from tail tips. Primers to amplify the wild type and targeted *Xpd* allele, as well as primer sequences for *lacZ* determination have been described previously [18,19].

2.2. Experimental design

Mice were marked and randomized at the day of birth in nine different groups, i.e. the longevity cohort, or one of the interim cohorts in which the mice were sacrificed at a fixed age of 2, 6, 13, 26, 52, 78, 91, 104, 117 or 130 weeks, respectively (scheduled sacrifice). The interim cohorts consisted of 15 Xpd^{TTD} mice, as well as 15 C57BL/6 control animals per sex per time point. In the longevity cohort, a total of 45 Xpd^{TTD} and 45 C57BL/6 controls per sex were monitored during their entire life span. Additionally, a sub-cohort of 30 wild type Xpd^{TTD} littermate controls was examined in a parallel longevity study to compare survival, pathology and body weight with the true C57BL/6 cohort. In the present study, only the findings of female Xpd^{TTD} and C57BL/6 animals are reported because data obtained with female Xpd^{TTD} wild type littermates were very similar to those from female C57BL/6 mice (data not shown). Furthermore, results from male Xpd^{TTD} and C57BL/6 mice were comparable to those from females (data not shown). The health state of the mice was checked daily, beginning at the day of weaning. Individual animals were weighed biweekly to determine live weights. All animals were kept during their entire life span in the same and stringently controlled environment, fed ad libitum under a normal day/night rhythm. The microbiological status of the cohorts was monitored every 3 months during the entire study. Food intake was determined in a subgroup of 10 individual animals per genotype. Animals from the longevity

cohort were removed from the study only when found dead or moribund. Complete autopsy was performed on animals of all cohorts; a total of 45 different tissues was isolated from each animal and stored for further analysis. Total animal weights as well as various organ weights were determined at time of death.

2.3. Pathology

Organ samples (40 organs and tissues) of intact animals and dissected for histopathology, were preserved in a neutral aqueous phosphate-buffered 4% solution of formaldehyde (10% neutral buffered formalin). In addition, samples of 17 different organs were snap-frozen in liquid nitrogen for further molecular biological analyses (to be published elsewhere). Tissues required for microscopic examination were embedded in paraffin wax, sectioned at 5 μm and stained with haematoxylin and eosin. Kidneys were also stained with Periodic Acid Schiff (PAS) and unstained slides were prepared of liver, brain, adrenal, ovaries and heart for lipofuscin UV-fluorescence determination. Other staining methods were used incidentally if necessary. Detailed microscopic examination was performed on all organs and tissues of all female Xpd^{TTD} and C57BL/6 control mice. Histopathological abnormalities were recorded using the PATHOS pathology data acquisition software and if possible, a cause of death was established for each animal.

2.4. Statistical evaluation

Statistical analyses of mortality curves included calculation of Kaplan–Meier distributions of survival of the two different genotypes and comparison by a two-sided Log rank test (SPSS, Version 11). Also, cause of death (COD) was analyzed using the Kaplan–Meier survival statistics. Incidences of lesions and tumors were analyzed with the Fisher's exact test and with the method of Peto, respectively [20].

3. Results

3.1. Body weights and food intake

Xpd^{TTD} mice have a remarkable phenotype that clearly mimics a segmental progeroid syndrome (Fig. 1) [16]. One striking hallmark of adult Xpd^{TTD} mice is a reduced bodyweight. In order to get more knowledge on bodyweight kinetics during life, we determined biweekly the bodyweights of Xpd^{TTD} and control C57BL/6 female mice. Results of individual animals (live weights) are plotted in Fig. 2. From this graph it is clear that at early age, growth characteristics for the Xpd^{TTD} females were quite similar to those of C57BL/6 control females. However, when female mice reached the age of 13 weeks, striking differences in body weight gain became apparent between Xpd^{TTD} and C57BL/6

Fig. 1. Age-matched Xpd^{TTD} and C57BL/6 mice of ∼90 weeks old. On the left, a C57BL/6 mouse and right a Xpd^{TTD} mouse which is much smaller and tinier. Also, brittle hair and skin lesions are clearly visible.

females, which persisted during the rest of their lives. In general, C57BL/6 females gained weight until the age of 86–90 weeks with a mean weight of 39.0 ± 6.2 g. After the age of 90 weeks, the majority of the wild type animals started to loose weight to a mean weight of about 32.0 g at the time of death. Body weights of female Xpd^{TTD} wild type littermates were comparable to those of the C57BL/6 controls (data not shown). Xpd^{TTD} females however, remained low in weight during their entire life span. The mean weight was about 25 g from the age of 36 weeks until 90 weeks, showing a remarkable tight distribution for over a 1.5–2-year period. Also, Xpd^{TTD} female body weights displayed a tendency to decline in the final weeks of their life and as can be expected from mice with a lower body weight and diminished fat reserves; this drop was not as pronounced as observed in C57BL/6 mice. Average weight at the time of death in Xpd^{TTD} females was 23.3 ± 2.5 g. Importantly, the difference in body weight between Xpd^{TTD} and C57BL/6 mice could not be explained

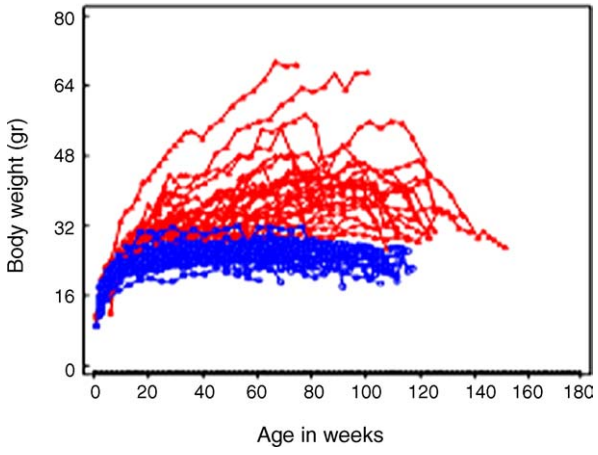

Fig. 2. Body weight curves of Xpd^{TTD} and C57BL/6 female mice during life. Weights of Xpd^{TTD} females are depicted in blue, weights of C57BL/6 control females in red. (For interpretation of the references to color in this figure legend, the reader is referred to the web version of the article.)

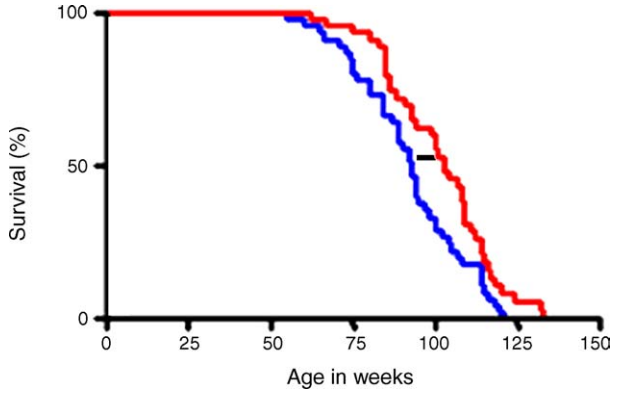

Fig. 3. Survival curves of Xpd^{TTD} (blue) and C57BL/6 (red) female mice. A statistical significant difference was determined using Kaplan–Meier survival statistics with Log rank test: p-value = 0.0163. (For interpretation of the references to color in this figure legend, the reader is referred to the web version of the article.)

by a difference in food intake as determined in a sub-cohort of female mice during the first 26 weeks of life. Both Xpd^{TTD} females and C57BL/6 control mice consumed 30–35 g of food per week during this period (data not shown).

3.2. Survival of Xpd^{TTD} and C57BL/6 female mice

The survival curves for the aging cohorts of female Xpd^{TTD} as well as C57BL/6 mice as presented in Fig. 3 are based on 45 animals per genotype. All animals were removed from the cohort when found dead or when they appeared moribund. In Table 1, the age of each group at 50% survival (median survival) and maximal survival (mean age of the oldest 20%) are summarized, and the age of the oldest survivor of each genotype is listed. The median survival of Xpd^{TTD} females (93 weeks) appeared significantly reduced ($p = 0.0163$, Kaplan–Meier with Log rank test) compared to the median survival of the C57BL/6 wild type controls (103 weeks). Also, the average of the longest-lived 20% of the Xpd^{TTD} cohort was lower than in C57BL/6 females, as well as the age of the oldest survivor (Table 1). Again, survival curves of Xpd^{TTD} wild type littermates were comparable to those of C57BL/6 controls (data not shown).

3.3. Organ weights

Analysis of organ weights in groups of animals with considerably different growth and terminal body weights is complicated. Absolute and relative organ weights should be evaluated together and in conjunction with body weights. Presented are the organ weights of scheduled interim sacrifices, since these weights give a good impression of the trends in organ weights in time in relatively healthy animals not suffering from terminal diseases. The absolute brain weight (Fig. 4A) was within a narrow range and was only slightly lower in Xpd^{TTD} mice compared to C57BL/6 control females. In contrast to the relatively stable brain weight, the other organs weights determined (heart, kidney, liver, spleen and thymus) are known to be influenced by variations in growth, diet, physiology or health status. Therefore, relative weights are more informative for these organs (Fig. 4B–F). Evaluation of the lymphoid organs revealed a considerable decrease in relative (and absolute) thymus weights during life in WT mice as expected and consistent with aging, but this decline was distinctly more pronounced in Xpd^{TTD} females (Fig. 4B). The relative spleen weights of both genotypes (Fig. 4C) tended to increase in time and were higher in Xpd^{TTD} than in C57BL/6 mice up to 78 weeks but decreased afterwards in Xpd^{TTD} mice only. The Xpd^{TTD} females showed a higher variation in splenic weight, which is probably due to increased extramedullary hematopoiesis in many animals, whereas others showed lymphoid depletion. The kidney increased in weight over the whole lifespan in both genotypes and relative kidney weights were higher in Xpd^{TTD} than in C57BL/6 mice (Fig. 4D). This implies that the kidney weight stays high while the overall body weight declines, due to loss of subcutaneous and abdominal fat by Xpd^{TTD} females (see below). The heart weights of all mice increased over the whole experimental period and surprisingly not only the relative but also the absolute heart weights were higher in Xpd^{TTD} mice when compared to the C57BL/6 controls, despite the low body weights (Fig. 4E). Liver weights in female mice increased in C57BL/6 mice during aging, whereas the liver weights remained more or less the same in Xpd^{TTD} mice over time (Fig. 4F). In summary, the weights of heart, kidney and spleen appeared to be higher and thymus weights were lower in Xpd^{TTD} females when compared to C57BL/6 controls.

Table 1
Survival curve summary female mice

	C57BL/6	Xpd^{TTD}
50% Survival[a]	103	93
20% Survival[b]	121	115
Oldest survivor[c]	133	121

[a] Median survival in weeks (first week of 50% mortality).
[b] The average of the longest-lived 20% of a cohort in weeks.
[c] Age in weeks.

3.4. Hematological findings

In keeping with our previous findings [16], Xpd^{TTD} mice showed reduced red blood cell counts (RBC) during their whole life span. For instance, RBC values were 7.4, 6.4 and 7.6×10^{12} cells/l for Xpd^{TTD} mice and 8.6, 8.4 and 8.3×10^{12} cells/l for C57BL/6 controls at the age of 52, 78 and 104 weeks, respectively. This RBC decrease in mutant mice was associated with decreased hemoglobin and hematocrit values. However, the mean cellular hemoglobin concentration (MCHC) as well as mean corpuscular volume (MCV) was not altered in Xpd^{TTD} mice versus the C57BL/6 controls (data not shown), pointing to a mild normochrome anemia in Xpd^{TTD} mice. Platelets increased initially in both genotypes and were relatively high in Xpd^{TTD} females but decreased after the age of 78 weeks (from 1392 to 1151 at the age

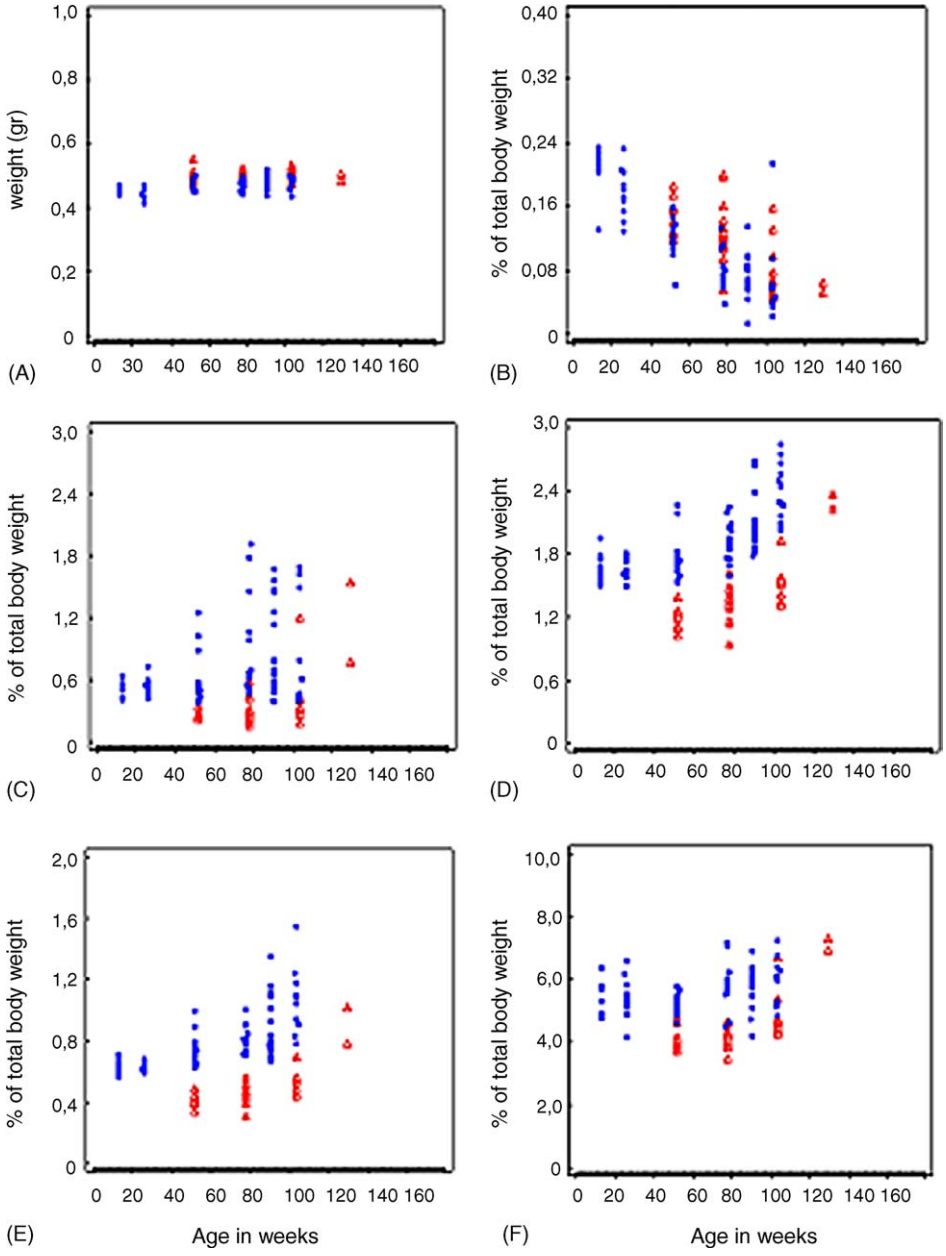

Fig. 4. Organ weights at time of schedules sacrifice. (A) Absolute brain weight in grams. Relative weights (as % of total weight) of thymus (B), spleen (C), kidney (D), heart (E) and liver (F). Organ weights of Xpd^{TTD} females are depicted in blue, organ weights of C57BL/6 control females in red. (For interpretation of the references to color in this figure legend, the reader is referred to the web version of the article.)

of 104 weeks). The amount of white blood cells showed a considerable variation over the whole experimental period in both genotypes (data not shown).

3.5. Causes of death

In Table 2, the causes of death are listed for both Xpd^{TTD} and C57BL/6 control mice as determined by combined gross and microscopic pathology. It is clear from this table that striking differences exist between the two genotypes. While in C57BL/6 control females most of the mice died of neoplasms (35%) and (skin) inflammation (50%), these numbers were much lower in the *Xpd* mutant mice (20 and 6%, respectively). In contrast, the most common cause of death in Xpd^{TTD} mice was anorectal prolapse (34%) or a general conditional decline without major pathological conditions that could be designated as a primary cause of death or a reason for the moribund state (31%). These phenomena were hardly found in the wild type controls (0 and 8%, respectively). Using the Kaplan–Meier survival statistics, both decrease in (skin) inflammation ($p < 0.01$) and increase in anorectal prolapse or conditional decline ($p < 0.001$) were statistically

Table 2
Causes of death in Xpd^{TTD} and C57BL/6 mice

	C57BL/6		Xpd^{TTD}	
	$n = 40$	%	$n = 35$	%
Neoplasms	14	35	7	20
Inflammation	20	50	2	6*
Multiple pathology	0	0	2	6
Prolaps	0	0	12	34**
Circulatory disorders	2	5	0	0
Conditional decline	3	8	11	31**
Other	1	3	1	3

N.B. A cause of death was only given when complete autopsy and full histopathology was performed. Autolysed mice were excluded. Statistically significant difference using Kaplan–Meier survival statistics $^{*}p < 0.01$ and $^{**}p < 0.001$.

significant. However, the decrease of neoplasms as a cause of death observed in the Xpd^{TTD} mice did not reach the level of statistical significance (see also next section).

3.6. Tumor development during aging

A summary of tumor incidence in old female C57BL/6 wild types and Xpd^{TTD} mice at the time of death is shown in Table 3A. From Table 2 it becomes clear that wild type mice mostly died of neoplasia (fatal tumors) while for Xpd^{TTD} mice other diseases were more life threatening (see above). However, mice of both genotypes showed occult tumors that were not the actual cause of death, but were found incidentally in mice dying of another cause (incidental tumors). In Table 3A, when Xpd^{TTD} females were compared with C57BL/6 control mice at the time of death, both the total number of benign and malignant tumors appeared to be lower in Xpd^{TTD} mice. This indicates that there is no difference in tumor progression between the two genotypes. The percentage of tumor-bearing animals (54.3% versus 75%) and the mean number of tumors per mouse (0.6 versus 1.0) appeared to be lower in Xpd^{TTD} mice when compared to wild type controls. Also, as Xpd^{TTD} mice live shorter, the tumors were found earlier than in wild type controls (mean latency time of 699 and 788 days, respectively). However, although there is a clear trend for lower tumor frequencies in Xpd^{TTD} mice, at present no firm conclusion on significant differences in cancer proneness between genotypes can be drawn. For that, further pathology analyses on cross sectional kills are needed.

Table 3A
Tumor development in Xpd^{TTD} and C57BL/6 mice at the time of death: tumor summary in female mice

	C57BL/6		Xpd^{TTD}	
	$n = 40$	%	$n = 35$	%
Number of benign tumors	24		12	
Number of malignant tumors	18		10	
Total number of tumors	42		22	
Mean number of tumors per mouse	1.1		0.6	
Number of tumor bearing animals	30	75.0	19*	54.3
Number of multiple tumor bearers	12	30.0	3	8.6
Median latency (50% percentile)[a]	788		699	

Mean age at time of death for the mice analyzed is 99.6 weeks for C57BL/6 and 90.8 weeks for Xpd^{TTD} mice.
[a] Median tumor latency in days.
* $p = 0.10$ (Fisher exact test two-sided) and not significant with the Peto method.

Table 3B
Tumor development in Xpd^{TTD} and C57BL/6 mice at the time of death: individual tumor types

		C57BL/6	Xpd^{TTD}
		$n = 40$	$n = 35$
Adrenal	Pheochromocytoma (benign)	0	3
Bone	Osteosarcoma	2	0
Head	Squamous cell carcinoma	0	1
Harderian gland	Adenoma	1	0
Lymphatic system	Lymphoma	10	3*
	Histiocytic sarcoma	3	3
Liver	Hepatocellular carcinoma	0	1
	Sarcoma	1	0
Lung	Bronchiolo-alveolar carcinoma	0	1
Pituitary	Pars distalis adenoma	20	3**
Small intestines	Leiomyosarcoma	1	0
Skin	Melanoma (benign)	0	1
Thyroid	Follicular cell adenoma	1	2
Vascular system	Hemangioma	2	3
	Hemangiosarcoma	1	1

Mean age at time of death for the mice analyzed is 99.6 weeks for C57BL/6 and 90.8 weeks for Xpd^{TTD} mice. Statistically significant difference using Fisher's exact test $^{*}p < 0.05$ and $^{**}p < 0.001$. Statistically significant difference using method of Peto $^{**}p = 0.002$. Incidences of all other tumors are too low to reveal statistically significant differences.

Incidences of the individual tumor types at the time of death are summarized in Table 3B. All tumors belonged to the spectrum normally observed in aging C57BL/6 mice. The incidences of the majority of these tumors were too low (less than 5%) to reveal any significant differences between the genotypes. As expected, only lymphomas and pituitary pars distalis adenomas had a relatively high incidence in C57BL/6 females and appeared to have a distinctly lower incidence in Xpd^{TTD} mice (Table 3B). These differences were statistically significant for both lymphomas ($p = 0.05$) and pituitary adenomas ($p < 0.001$, Fisher's exact test). However, when the data were corrected for differences in survival, using the Peto method [20], only the incidence of pituitary adenomas, but not lymphomas, was statistically significantly decreased in Xpd^{TTD} mice ($p = 0.002$ and $p = 0.26$ two-sided, respectively).

3.7. Non-neoplastic pathology

In addition to tumors, both C57BL/6 and Xpd^{TTD} mice showed a large variety of non-neoplastic pathological abnormalities in several organ systems: inflammatory, proliferative, degenerative or regressive. Many of these abnormalities are known to increase with age in C57BL/6 wild type mice. Most of these lesions occurred to about the same degree and incidence in both genotypes and will not be discussed here any further. In addition, pathology features in Xpd^{TTD}

Table 4
Histopathology differences in Xpd^{TTD} and C57BL/6 mice at the time of death

	C57BL/6 ($n = 40$)		Xpd^{TTD} ($n = 35$)	
	Incidence	Severity	Incidence	Severity
(A) Differences consistent with accelerated aging				
Osteoporosis femur	88.2	3.3	97.1	4.1
Hepatic lipofuscin accumulation	85.0	1.6	97.1	3.1
Hepatic intranuclear inclusions	10.0	0.1	28.6	0.5
Hepatocellular atrophy	5.0	0.1	34.3	0.5
Renal karyomegaly	17.9	0.2	38.2	0.7
Renal tubular dilatation	30.8	0.5	85.3	2.2
Renal hyaline glomerulopathy	15.4	0.3	52.9	1.1
Aortic sarcopenia	5.6	0.1	87.9	2.0
Lymphoid depletion spleen	30.8	0.4	85.7	2.0
Lymphoid depletion thymus	82.8	2.6	100	3.7
Skin reduced hypodermal fat	18.9	0.5	85.7	2.9
Heart lipofuscin accumulation	100	1.9	100	2.3
(B) Trichothiodystrophy-specific differences				
Anorectal prolapse	0	n.a.	51.4	n.d.
Duodenal atypical hyperplasia	0	n.a.	17.6	0.5
Skin ulcerative dermatitis	45.9	1.5	8.6	0.3
TTD skin lesions[a]	0	n.a.	Increased	n.d.
(C) Differences consistent with dietary restriction				
Skin ulcerative dermatitis	45.9	1.5	8.6	0.3
Skin reduced hypodermal fat	18.9	0.5	85.7	2.9
Cataract of eye lens	42.1	0.7	9.1	0.1
Nerve demyelination	59.0	1.1	11.8	0.1
Pituitary adenoma	51.3	n.a.	8.6	n.a.
Thyroid follicular cell hyperplasia	21.6	0.4	5.9	0.1
Thyroid follicular distension (“cold follicles”)	94.6	2.6	85.7	1.9
Inflammation in various organs			Decreased	
Lacrimal gland lipofuscin accumulation[b]	94.3	1.7	46.9	0.5
Lacrimal gland Harderian type acini[b]	57.1	1.3	21.9	0.4
Adrenal extramedul hematopoiesis[b]	45.0	1.0	34.3	0.6
Brain eosinophilic inclusions thalamus[b]	55.0	1.0	34.0	0.6

Incidences are determined at the time of death and given in %, severity in a score (scale 1–5), mean severity is calculated per group; Mean age at time of death for the mice analyzed is 99.6 weeks for C57BL/6 and 90.8 weeks for Xpd^{TTD} mice. n.a., not applicable; n.d., not determined.

[a] TTD skin lesions is an assembly of acanthosis, hyperkeratosis, sebaceous hyperplasia, mast cell infiltration, extra-cellular melanin and follicular distention. No quantitative grade of severity is depicted for the separate features.

[b] Possibly consistent with dietary restriction (not found in literature).

wild type littermates were found to be comparable to those in C57BL/6 females (data not shown). Several abnormalities showed biological (and statistical) relevant differences in incidence and/or severity between Xpd^{TTD} and C57BL/6 mice. These differences can be subdivided into various categories as pointed out below (see also Table 4).

3.7.1. Accelerated aging features

Histopathological features of this category were consistent with and added on the earlier described premature aging phenotype of the Xpd^{TTD} mice [16]. Age-related pathology at the time of death was found to be most overt in liver, kidney, bone as well as lymphoid tissues (Table 4A; Fig. 5A). Lipofuscin accumulation in the liver was distinctly most severe in Xpd^{TTD} females (Fig. 5A-III). The age-related pigment was present mainly in Kupffer cells, but also in hepatocytes. A similar trend was present in the heart of Xpd^{TTD} mice, although to a lesser extent. Eosinophilic or ‘empty’ hepatic intra-nuclear inclusions occurred to a higher extent in Xpd^{TTD} than in C57BL/6 mice. Hepatic intra-nuclear inclusions increase with age and are generally considered to be invaginations of the nuclear membrane containing cytoplasm [21]. Renal karyomegaly, seen as large, frequently bean-shaped nuclei in epithelial cells of the pars recta of the proximal renal tubules was slightly more pronounced in Xpd^{TTD} mice. Furthermore, the renal tubules were frequently dilated, which might be the cause of the high relative kidney weights of Xpd^{TTD} mice. Renal hyaline glomerulopathy occurred generally to a mild degree in C57BL/6 mice, but was much more pronounced in Xpd^{TTD} females (Fig. 5A-II). Evidence for the occurrence of osteoporosis of the femur, characterized by loss of trabecular bone, as well as kyphosis (although not quantified) was found in Xpd^{TTD} mice (Table 4; K. Diderich et al., in preparation). The increase of lymphoid depletion of the spleen in Xpd^{TTD} females was characterized by a decreased lymphocytic density and a smaller extent of the splenic white pulp area. This may provide an explanation for the decline in spleen weight observed later in life for the Xpd^{TTD} mutant

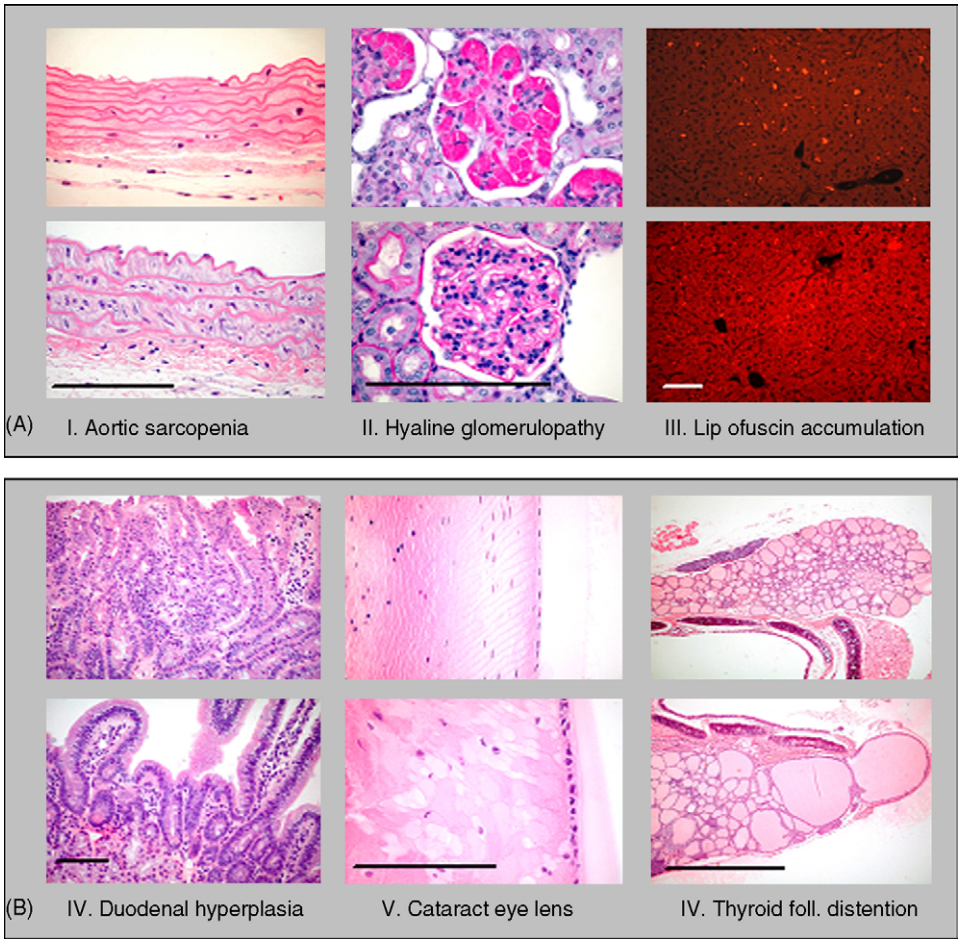

Fig. 5. Examples of histopathology differences between Xpd^{TTD} and C57BL/6 female mice. Examples of age-related (A-I–III), TTD-specific (B-IV) and caloric-restriction-related differences (B-V, VI) are depicted. The upper picture of every set is of an Xpd^{TTD} mouse, the lower picture of a C57BL/6 mouse.Age-related pathology differences: (I) aortic sarcopenia in an Xpd^{TTD} female (644 days) and C57BL/6 mouse (662 days). Note the scarcity of nuclei between the elastic fibers in the Xpd^{TTD} aorta. (II) Kidney hyaline glomerulopathy in an Xpd^{TTD} female (497 days) and C57BL/6 mouse (722 days). PAS-positive purple stained deposits (negative for amyloid) within glomeruli of the Xpd^{TTD} kidney that were absent in the C57BL/6 control kidney. (III) Lipofuscin fluorescence (UV) in the liver of an Xpd^{TTD} mouse (735 days), which was distinctly less in a C57BL/6 female (855 days). (IV) TTD-specific atypical epithelial hyperplasia of the duodenum at the gastroduodenal junction. Note the crowding of nuclei and the disorganized aspect in the Xpd^{TTD} duodenum (735 days). Normal duodenum of a C57BL/6 mouse (624 days) is shown for a clear comparison.Dietary restriction-related pathology differences: (V) cataract of the eye lens of a C57BL/6 mouse (722 days), note the swollen and vacuolated lenticular fibers. The lens of the Xpd^{TTD} female (659 days) is relatively normal. (VI) Thyroid with distended follicles in a C57BL/6 female (764 days) and normal-sized follicles in a Xpd^{TTD} female (609 days).Pictures were obtained using HE staining (I, IV, V, VI) or PAS-staining (II). For III, unstained slides were used. Magnification bars shown represent 0.1 mm in all pictures (except the thyroid (VI): 1 mm). Upper and lower picture in one panel show the same magnification. Objectives used were 5× (VI), 20× (III, IV) or 40× (I, II, V).

mice. The normal age-related involution (lymphoid atrophy) of the thymus, with loss of organoid structure and decrease in size, was more pronounced in Xpd^{TTD} than in C57BL/6 mice and correlated with the decreased organ weights. Aortic sarcopenia was defined as loss of muscle cells in the tunica media, a condition that occurred almost exclusively in Xpd^{TTD} mice (Fig. 5A-I). Since the number of muscle cells in aortas of 3 and 6 months old Xpd^{TTD} mice did not differ from those of age-matched C57Bl/6 controls (data not shown), aortic sarcopenia should be considered as a real aging-related phenomenon. Another conspicuous feature, specifically present in aging Xpd^{TTD} mice, was reduced or absent hypodermal fat as compared to C57BL/6 mice of the same age. This explains the consistent lower body weights of the Xpd^{TTD} animals.

3.7.2. Xpd^{TTD}-specific features

The second category of pathology differences consisted of differences specifically for the TTD phenotype that manifest during the whole lifespan (Table 4B; Fig. 5B). One of the most striking hallmarks of TTD patients is the brittleness of hair as was also found in Xpd^{TTD} mice. In more detail, Xpd^{TTD} mice showed acanthosis, hyperkeratosis, sebaceous gland hyperplasia, mast cell infiltration, extra-cellular melanin and follicular distention in the skin (mentioned as TTD skin lesions in Table 4B). Duodenal epithelial hyper-

plasia just near the gastro-duodenal junction occurred mainly in Xpd^{TTD} mice (Fig. 5B-IV). However, no intestinal tumors were observed in this area in any of the mice. A striking feature of Xpd^{TTD} mice in our study was anorectal prolapse, a condition in which a part of the rectum protrudes through the anus. Since this change was followed by perianal inflammation and ulceration it was a frequent cause of death of Xpd^{TTD} mice (see above). The non-protruding part of the rectal mucosa of affected animals appeared not to be altered, however. No evidence of inflammation of the large intestines was found, a condition that has been associated before with rectal prolapse [22]. In conclusion, the observed anorectal prolapse in Xpd^{TTD} mice is probably associated with the prolonged cachectic state of the mice or with Xpd^{TTD}-specific changes in the perianal musculature and as such there is no relationship with aging per se.

3.7.3. Signs of caloric restriction

Apart from the aging-related changes and Xpd^{TTD}-specific changes, we found a third unexpected category of altered (reduced) pathology in Xpd^{TTD} mice at the time of death, consistent with a phenotype associated with dietary/caloric restriction (CR)(Table 4C; Fig. 5B). These features include a considerably lower incidence and/or severity in Xpd^{TTD} mice of the following symptoms: de-myelination of the peripheral nerve, cataract (Fig. 5B-V), thyroid follicular distension (Fig. 5B-VI), pituitary adenomas, ulcerative dermatitis, etc. (see for further details Table 4C). Most of these abnormalities are known to increase during aging, but under conditions of CR they have been reported to occur with lower incidence and severity [23]. Also, age-associated reduction of hypodermal fat has been related to CR in rodents [23,24].

4. Discussion

Aging is poorly defined at the mechanistic level, because aging is pleiotropic and segmental in its nature. It is a complex process with concurrence of multiple diseases or disabilities on a background of increasing functional decline and failure of homeostasis, associated with reduced stress resistance and an increased risk of dying. The universal driver of the aging process, across species, is likely the accumulation of somatic damage in cellular macromolecules, such as DNA, with ROS as the prime suspect for being the main damage-inducing agent. In view of the importance of DNA as the ultimate template and the discovery that heritable mutations in DNA maintenance genes underlie almost all known human segmental progeroid syndromes, maintenance of genome integrity has now emerged as a major factor in longevity and cell viability. Mice are good model systems to investigate the molecular basis of (accelerated) aging, because of their powerful genetics and the similarity of genomes and genome maintenance systems between mice and man. Many mouse mutants defective in genome maintenance display, like their human counterparts, segmental progeria [14].

In order to further understand the causal relationship between the aging process and genome maintenance, we are currently performing complete life span studies with various mouse models harboring defects in one or both sub-pathways of the NER system (i.e. *Xpa*, *Csb*, *Xpc* and Xpd^{TTD} mice). In the present study, we focused on the Xpd^{TTD} mouse mutant, previously shown to display a segmental premature aging phenotype [16] that in retrospect could also be recognized in human trichothiodystrophy patients [12]. A cohort of female Xpd^{TTD} mice was compared under strict SPF conditions to control mice having the same C57BL/6 genetic background. Such a side-by-side comparison with the normal aging process is the only valid way of identifying genuine symptoms of premature aging [3].

4.1. TTD is a segmental progeroid disorder

From present and previous results, it appears that the Xpd^{TTD} mice, just like the TTD patients, display wide-spread, premature segmental multi-system aging. Xpd^{TTD} mice show accelerated aging for a large number of known aging parameters (Table 4A) and as such they are excellent to study various (not all) premature aging phenotypes. When assumed that the underlying mechanism of aging in Xpd^{TTD} mice is similar as that in normal aging, this mouse model could be of potential use in future intervention studies.

Although a statistically significant difference in life span between Xpd^{TTD} mice and C57BL/6 control mice was observed, Xpd^{TTD} mice in the present study lived significantly longer than reported initially [16]. The major differences between these two studies were differences in genetic background and housing conditions. Either one of these can have impact on the ultimate outcome of longevity studies and underline that genuine comparison of the life span of different strains can only be reliably done under such strict conditions. An important cause of death in Xpd^{TTD} mice, and not in C57BL/6 controls, was a general conditional decline (including cachexia), also found in TTD patients [12]. Perhaps this state of conditional decline should be considered as a failure of the organism to maintain homeostasis. Additional causes of death were anorectal prolapse in Xpd^{TTD} mice and inflammation (mainly ulcerative dermatitis) in C57BL/6 mice, which was also reported by others [25,26].

In TTD patients, a specific form of anemia (thalassaemia, trait) has been described [27] that has been related to reduced levels of transcription of the *β-globin* gene. Although the type of anemia observed in Xpd^{TTD} mice (normochrome) appears to be slightly different from that in TTD patients, a similar etiology may be postulated. Pronounced kyphosis and evidence for osteoporosis were found in aging Xpd^{TTD} mice, pointing to age-related skeletal abnormalities as were also found in TTD patients [12]. In addition to these known age-related features, the detailed systematic analysis performed in the present study revealed new (histo-) pathological parameters of aging in various organs and tissues of Xpd^{TTD} females. Especially lipofuscin accumulation in liver (and heart) cells

was a very interesting observation since the accumulation of this pigment can be associated with oxidative damage [28], underlining the theory that defects in genome maintenance may be directly related to accumulating aging features. However, as the XPD protein functions both in DNA repair and transcription (initiation), it needs to be established whether the observed lipofuscin accumulation is due to defects in global genome NER, damage-induced interference of transcription by TCR or inactivated or constitutive transcription initiation of RNA polymerase I and II promoters. Also, renal karyomegaly has been associated with accumulation of DNA damage (M. Luijten et al., in preparation). One of the most pronounced age-related pathological differences between old Xpd^{TTD} and control females was aortic sarcopenia. This loss of aortic muscle cells was particularly enhanced in old mice. This loss together with the age-related growth retardation and skeletal abnormalities in Xpd^{TTD} mice, underlines the hypothesis that TTD is not a developmental disorder, but is truly due to early onset of specific aging-related symptoms.

Besides these genuine progeroid features of Xpd^{TTD} mice, we also found (TTD-related) features that do not meet age-related criteria. These are (i) the TTD-specific aberrant brittle hair and skin abnormalities; (ii) increase of duodenal atypical hyperplasia; (iii) anorectal prolapse probably as a consequence of the cachectic state of the mice. It is our hypothesis that these TTD-specific features are caused by a transcriptional deficit rather than by a defect in the DNA repair function of the XPD protein.

4.2. Xpd^{TTD} mice show signs of caloric restriction

A striking finding in the present study, purely based on pathological findings, was the identification of CR features in Xpd^{TTD} mice. Pronounced effects of CR on a variety of pathological abnormalities as well as mean and maximum life span in mammalian species are well documented [29,30]. In C57BL/6 mice on a restricted diet, the frequency of pituitary adenomas as well as dermatitis, other inflammatory changes and cataract appears considerably reduced [23]. The following observations in Xpd^{TTD} mice are in line with this CR hypothesis: (i) a low body weight accompanied by low hypodermal fat mass and absence of abdominal fat; (ii) reduced tumor development; (iii) low frequency of inflammation and cataract.

Strikingly however, food intake of Xpd^{TTD} mice was comparable to that of the wild type C57BL/6 mice, indicating that the CR phenotypes may be due to metabolic problems in Xpd^{TTD} mice owing to mild transcription failures. Supportive to this assumption are our preliminary data on mouse models with true NER defects like *Xpa* and *Xpc*, which lack such an apparent CR phenotype (to be published elsewhere). Definite proof that Xpd^{TTD} mice go into a state of metabolic restriction should come from more dedicated studies like biochemical analyses (for instance glucose, insulin, IGF-1 [31]), studies that were not possible to combine with our current longevity experiment. Still though, preliminary micro-array analyses further support our CR hypothesis (Suh et al., manuscript in preparation).

In conclusion, it is conceivable to assume that inefficient energy uptake is advantageous to Xpd^{TTD} mice. Under such conditions, production of harmful metabolic side products (like ROS) will be decreased which is in favor of DNA-repair deficient Xpd^{TTD} mice, and clearly more general to all living organisms when survival is considered.

Acknowledgements

We are very grateful to Piet de With, Gwen Intres, Conny van Oostrom, Coen Moolenbeek, Christine Soputan and Henny Loendersloot for their skilful technical assistance. This work was financially supported by National Institute of Health (NIH)/National Institute of Aging (NIA), grant number 1 PO1 AG-17242, NIEHS (1UO1 ES011044), Netherlands Organization for Scientific Research (NWO) through the foundation of the Research Institute Diseases of the Elderly, as well as grants from the Dutch Cancer Society, (EUR 99-2004) and EC (QRTL-1999-02002).

References

[1] R.G. Allen, A.K. Balin, Metabolic rate, free radicals and aging, in: R.G. Cutler, H. Rodriguez (Eds.), Oxidative Stress and Aging. Advances in Basic Science, Diagnostics and Intervention, vol. I, World Scientific Publishing, Singapore, 2003, pp. 3–23.
[2] L. Partridge, D. Gems, Mechanisms of ageing: public or private? Nat. Rev. Genet. 3 (2002) 165–175.
[3] P. Hasty, J. Vijg, Accelerating aging by mouse reverse genetics: a rational approach to understanding longevity, Aging Cell 3 (2004) 55–65.
[4] D. Harman, Aging: a theory based on free radical and radiation chemistry, J. Gerontol. 11 (1956) 298–300.
[5] T. Finkel, N.J. Holbrook, Oxidants, oxidative stress and the biology of ageing, Nature 408 (2000) 239–247.
[6] J. Cadet, M. Berger, T. Douki, J.L. Ravanat, Oxidative damage to DNA: formation, measurement, and biological significance, Rev. Physiol. Biochem. Pharmacol. 131 (1997) 1–87.
[7] J.H.J. Hoeijmakers, Genome maintenance mechanisms for preventing cancer, Nature 411 (2001) 366–374.
[8] E.C. Friedberg, G.C. Walker, W. Siede, DNA Repair and Mutagenesis, American Society of Microbiology, Washington, DC, USA, 1995.
[9] E. Evans, J.G. Moggs, J.R. Hwang, J.M. Egly, R.D. Wood, Mechanism of open complex and dual incision formation by human nucleotide excision repair factors, EMBO J. 16 (1997) 6559–6573.
[10] S.J. Araujo, F. Tirode, F. Coin, H. Pospiech, J.E. Syvaoja, M. Stucki, U. Hubscher, J.M. Egly, R.D. Wood, Nucleotide excision repair of DNA with recombinant human proteins: definition of the minimal set of factors, active forms of TFIIH, and modulation by CAK, Genes Dev. 14 (2000) 349–359.
[11] D. Bootsma, K.H. Kraemer, J.E. Cleaver, J.H.J. Hoeijmakers, Nucleotide excision repair syndromes: xeroderma pigmentosum, Cockayne syndrome and trichothiodystrophy, in: B. Vogelstein, K.W. Kinzler (Eds.), The Genetic Basis of Human Cancer, Mc-Graw-Hill Companies, USA, 1998, pp. 245–274.

[12] P.H. Itin, A. Sarasin, M.R. Pittelkow, Trichothiodystrophy: update on the sulfur-deficient brittle hair syndromes, J. Am. Acad. Dermatol. 44 (2001) 891–920.
[13] D.G. Martin, Genetic syndromes in man with potential relevance to the pathobiology of aging, in: Birth Defects, Original Article Series, vol. 14, The National Foundation, New York, 1978, pp. 5–39.
[14] P. Hasty, J. Campisi, J.H.J. Hoeijmakers, H. van Steeg, J. Vijg, Aging and genome maintenance: lessons from the mouse? Science 299 (2003) 1355–1359.
[15] J. de Boer, J.H.J. Hoeijmakers, Cancer from the outside, aging from the inside: mouse models to study the consequences of defective nucleotide excision repair, Biochimie 81 (1999) 127–137.
[16] J. de Boer, J.O. Andressoo, J. de Wit, J. Huijmans, R.B. Beems, H. van Steeg, G. Weeda, G.T.J. van der Horst, W. van Leeuwen, A.P.N. Themmen, M. Meradji, J.H.J. Hoeijmakers, Premature aging in mice deficient in DNA repair and transcription, Science 296 (2002) 1276–1279.
[17] E. Masoro, Role of sirtuin proteins in life extension by caloric restriction, Mech. Ageing Dev. 125 (2004) 591–594.
[18] J. de Boer, J. de Wit, H. van Steeg, R.J.W. Berg, H. Morreau, P. Visser, A.R. Lehmann, M. Duran, J.H.J. Hoeijmakers, G. Weeda, A mouse model for the basal transcription/DNA repair syndrome trichothiodystrophy, Mol. Cell 1 (1998) 981–990.
[19] M.E. Dollé, H. Giese, C.L. Hopkins, H.J. Martus, J.M. Hausdorff, J. Vijg, Rapid accumulation of genome rearrangements in liver but not in brain of old mice, Nat. Genet. 17 (1997) 431–434.
[20] R. Peto, M.C. Pike, N.E. Day, R.G. Gray, P.N. Lee, S. Parish, J. Peto, S. Richards, J. Wahrendorf, Guidelines for simple, sensitive significance tests for carcinogenic effects in long-term animal experiments, IARC Monogr. Eval. Carcinog. Risk Chem. Hum. 2 (Suppl.) (1980) 311–426.
[21] R.R. Maronpot, G.A. Boorman, B.W. Gaul (Eds.), Pathology of the Mouse, Cache River Press, Vienna, IL, USA, 1999.
[22] H. Takayama, H. Takagi, W.J. Larochelle, R.P. Kapur, G. Merlino, Ulcerative proctitis, rectal prolapse, and intestinal pseudo-obstruction in transgenic mice overexpressing hepatocyte growth factor/scatter factor, Lab. Invest. 81 (2001) 297–305.
[23] A. Turturro, P. Duffy, B. Hass, R. Kodell, R. Hart, Survival characteristics and age-adjusted disease incidences in C57BL/6 mice fed a commonly used cereal-based diet modulated by dietary restriction, J. Gerontol.: Biol. Sci. 57A (2002) B379–B389.
[24] E. Gursoy, A. Cardounel, Y. Hu, M. Kalimi, Biological effects of long-term caloric restriction: adaptation with simultaneous administration of caloric stress plus repeated immobilization stress in rats, Exp. Biol. Med. 226 (2001) 97–102.
[25] A.G. Andrews, R.C. Dysco, S.C. Spilman, R.G. Kunkel, D.W. Brammer, K.J. Johnson, Immune complex vasculitis with secondary ulcerative dermatitis in aged C57BL/6Nia mice, Vet. Pathol. 31 (1994) 293–300.
[26] B.-N. Blackwell, T.J. Bucci, R.W. Hart, A. Turturro, Longevity, body weight, and neoplasia in ad libitum-fed and diet-restricted C57BL/6 mice fed NIH-31 open formula diet, Toxicol. Pathol. 23 (1995) 570–582.
[27] V. Viprakasit, R.J. Gibbons, B.C. Broughton, J.L. Tolmie, D. Brown, P. Lunt, R.M. Winter, S. Marinoni, M. Stefanini, L. Brueton, A.R. Lehmann, D.R. Higgs, Mutations in the general transcription factor TFIIH result in beta-thalassaemia in individuals with trichothiodystrophy, Hum. Mol. Genet. 10 (2001) 2797–2802.
[28] D. Harman, Lipofuscin and ceroid formation: the cellular recycling system, Adv. Exp. Med. Biol. 266 (1989) 3–15.
[29] V.D. Longo, C.E. Finch, Evolutionary medicine: from dwarf model systems to healthy centenarians? Science 299 (2003) 1342–1346.
[30] E.J. Masoro, Subfield history: caloric restriction, slowing aging, and extending life, Sci. Aging Knowl. Environ. 8 (2003) RE2.
[31] M. Bluher, B.B. Kahn, C.R. Kahn, Extended longevity in mice lacking the insulin receptor in adipose tissue, Science 299 (2003) 572–574.